ISSN 0010-9525, Cosmic Research, 2017, Vol. 55, No. 5, pp. 338–344. © Pleiades Publishing, Ltd., 2017.
Original Russian Text © V.I. Kovalev, Yu.Ya. Ruzhin, Yu.A. Plastinin, B.A. Khmelinin, 2017, published in Kosmicheskie Issledovaniya, 2017, Vol. 55, No. 5, pp. 359–365.

Illumination of the Earth's Ionosphere by the Vacuum Ultraviolet Radiation Reflected by the Moon

V. I. Kovalev[a], †, Yu. Ya. Ruzhin[a], *, Yu. A. Plastinin[b], and B. A. Khmelinin[b]

[a] *Pushkov Institute of Terrestrial Magnetism, Ionosphere, and Radio Wave Propagation, Russian Academy of Sciences, Troitsk, Moscow, 142190 Russia*

[b] *Central Research Institute of Machine Building (TsNIIMash), Korolev, Moscow oblast, 141070 Russia*

**e-mail: vikov@izmiran.ru*

Received June 27, 2016

Abstract—The spectral curve of the flux density of the radiation, which is reflected by the full moon towards the Earth's ionosphere within a wavelength range of 200–1700 Å, has been presented. This curve is obtained by the approximation of space experiment data available in the scientific literature on the lunar spectral albedo and solar spectrum. Estimates of maximum values of spectral densities of fluxes reflected by the full moon in the neighborhood of wavelengths of ionization of basic ionospheric particles (neutral atoms of H I, He I, N I, O I, and Ar I and ions of He II, N II, O II, Ar II, N III, O III, and Ar III, as well as molecules of H_2, N_2, and O_2) are given.

DOI: 10.1134/S0010952517050069

1. INTRODUCTION

The interaction of the vacuum ultraviolet (VUV) radiation (wavelength $\lambda = 100–2000$ Å) with neutral atoms, ions, and molecules of the ionosphere have an influence on their energy states. In the VUV band, there are wavelengths that correspond to ionization energies, as well as to energies of highly excited (Rydberg) states of all the main ionospheric particles.

It is well known that part of the solar VUV radiation is reflected by the Moon to the Earth and, thus, can influence the ionosphere. To correctly set up and carry out space experiments aimed at studying weak artificial glows in the night ionosphere of the Earth using the onboard scientific instruments of the Russian segment of the *ISS*, e.g., in the Relaxation program [1], as well as the artificial aurora and substorm phenomena [2–6], the estimations of the radiant flux reflected by the Moon to the Earth within the entire VUV band are required.

The Moon was (and is) investigated thoroughly within a wide spectral range of wavelengths $\lambda > 2000$ Å in both ground-based observations and space experiments (see, e.g., [7–15]).

With regard to VUV radiation, it is completely absorbed by the surface layer of the atmosphere up to the altitude of the upper boundary of the ozone layer (~50 km). Therefore, the ground-based VUV-observations are impossible.

The modern data on the Moon characteristics in the VUV band are obtained as a result of unique measurements in individual narrow ranges of λ using the research apparatus of onboard complexes of space satellites and suborbital rockets. An explicit representation of the spectral irradiance curve of the radiation reflected by the Moon to the Earth in the entire VUV band is absent in the scientific literature.

A goal of our work is to approximate the radiation reflected by the Moon (in the phase of full moon) to the Earth's ionosphere in the range of 200–1700 Å using the he spectral irradiance curve based on the space experiment data available in the scientific literature on the spectral albedo of the Moon and on the solar spectrum, as well as to estimate the maximum values of radiant flux densities for wavelengths of the ionization of main ionospheric particles.

2. GEOMETRIC ALBEDO OF THE FULL MOON IN THE VUV BAND

The experiments carried out on the *Apollo 17* spacecraft [16] made it possible to measure the Moon's geometric albedo for the first time and to create a map of the lunar surface within a confined range of the far ultraviolet (FUV) band ($\lambda = 1220–2000$ Å).

In [17], a brief preliminary review of research results in the X-ray ($\lambda < 100$ Å), extreme-ultraviolet (EUV, $\lambda = 100–1210$ Å), and FUV bands is given, as well as the results of the exploration of the moon by scientific instruments of the *Extreme Ultraviolet*

† Deceased.

Explorer (EUVE) satellite are presented, namely, EUV images and EUV albedo of the Moon.

A main task of the EUVE satellite was the all-sky survey in the largest part of the wavelength range $\lambda <$ 911 Å. The scientific hardware comprised three scanning telescopes with photometers and a spectrometric telescope. The telescope photometers were equipped with filters that have a 10% passband in the ranges of 50–180, 160–240, 345–605, and 500–740 Å.

The sky investigations were performed over July 22, 1992 to January 22, 1993. The satellite observed the Moon several times in the first and last quarters and one day (December 10, 1992) under full-moon conditions following the lunar eclipse on December 9, 1992.

The satellite revolved along the orbit with a 96-min period, and three scanning telescopes covered great circles over the sky perpendicular to the Earth–Sun axis. The telescopes could observe the Moon in the first and last quarters of each month. The fields of view of two short-wave scanners were 5° in diameter, while the long-wave scanner had a field of 4°. The Moon was visible from the satellite orbit only for 20–25 s.

During the observation of several first and last quarters of the Moon, the satellite was positioned unfavorably according to a criterion of signal-to-noise ratio (S/N). Therefore, out of all the results obtained for presentation in [17], the authors have chosen the advents of two first quarters (August 5, 1992 and October 3, 1992) and two last quarters (September 19, 1992 and November 17, 1992), which had the best S/N ratio.

Upon correcting the results of observations of the first and last lunar quarters to the zeroth lunar phase (new moon) using the data of photometers, the lunar photometric function for the FUV band wavelengths [16], and the EUV91 solar spectrum model [18] with parameters specified for each particular observation period, the authors obtained average values of the geometric albedo of the full moon. They amounted to 0.15% (±0.03%), 3.1% (±0.3%), and 3.5% (±0.3%) for wavelength ranges of 150–240, 400–580, and 550–650 Å, respectively. The upper limit of the geometric albedo for a range of 75–180 Å was estimated to be 0.13%. The indicated standard deviations characterized only statistics of photon counting and did not take into account the additional errors introduced by the use of the EUV91 solar-flux model and procedure for correcting the phase angle correction.

In [17], it is stressed that, due to the absence of the EUV photometric function that is required for correcting the data obtained at phase angles of 90° to the data obtained at 0°, the FUV photometric function [16] was used based on the assumption that the correction factor in both bands is approximately the same and equal to 24.9.

The quantities $F_{10.7}$ and $\langle F_{10.7} \rangle$ in the EUV91 model [18], which characterize the solar activity, were equal to 131 and 127 as of Aug. 5, 1992, 113 and 121 as of Sept. 19, 1992, 119 and 124 as of Oct. 3, 1992, and 152 and 129 as of the date Nov. 17, 1992.

A total error of the results obtained is estimated as 30–50%. It is noted that the detected signals proved to be insufficient for the spatial analysis of the Moon image. The authors of [17] have shown that the EUV albedos of the Moon obtained and the previously published FUV-albedos correspond well to the reflection coefficients of SiO_2 and Al_2O_3 oxides.

Work [19], which presents the results of the full-moon observations by the onboard instruments of the EUVE satellite with significantly improved (in comparison to [17]) photometric characteristics, was published in 1998. Then, new spectroscopic results of observation and the novel images of the full moon were obtained, the first EUV maps of the lunar surface were constructed, and the lunar spectral reflectance was measured in the larger part of the EUV band. A detailed description of specific features of experiments, instruments, and methods for signal processing can be found in [19] and the references cited in it.

In work [19], the data on values of the geometric albedo of the full moon are given (Fig. 3), which were obtained in space experiments of *Apollo 17* [16], *Mariner 10* [20], *ROSAT/PSPC* [21], *EUVE* Survey [17], *Astro-2/HUT* [22], *ORFEUS-II/UCB* [23], and *EUVE* [19]. In total, the results of 30 measurements have been presented. According to the assessment of the authors of [19], the absolute error of the values obtained amounts to 30%.

The authors of [19] approximated the aggregate of the values of the geometric albedo of the full moon in the wavelength range of 140–1700 Å with a continuous curve that corresponds to the reflectance of the combination of oxides, i.e., 17% Al_2O_3 and 83% SiO_2 [24, 25]. This combination agrees well with the lunar volumetric composition of the oxides [26]. Any other oxides were not taken into account during the approximation because of absence of data for them on the reflectance in the EUV band.

Below, we analyze the spectral characteristics of the quantities under study, which belong to definite ranges of λ; i.e., they are quasi-monochromatic, rather than integral in λ. To reduce the text, we use the subscript λ to designate quantities, while the word *spectral* is omitted whenever possible. In the second letter in the subscript, the following notations are used: S is the Sun, M is the Moon, and I is the ionosphere.

We digitized the continuous curve from [19] that approximates the lunar albedo with the discreteness of 5 Å and an error of digitization on the order of 10% and constructed a graph of the spectrum of the geometric albedo of the full moon $p_{\lambda M}$. This is presented in Fig. 1 for the range λ = 200–1700 Å.

Dashed curves in Fig. 1 indicate the boundaries of the domain of errors of our estimates of $p_{\lambda M}$. The error of the $p_{\lambda M}$ values is ~35% with allowance for errors of

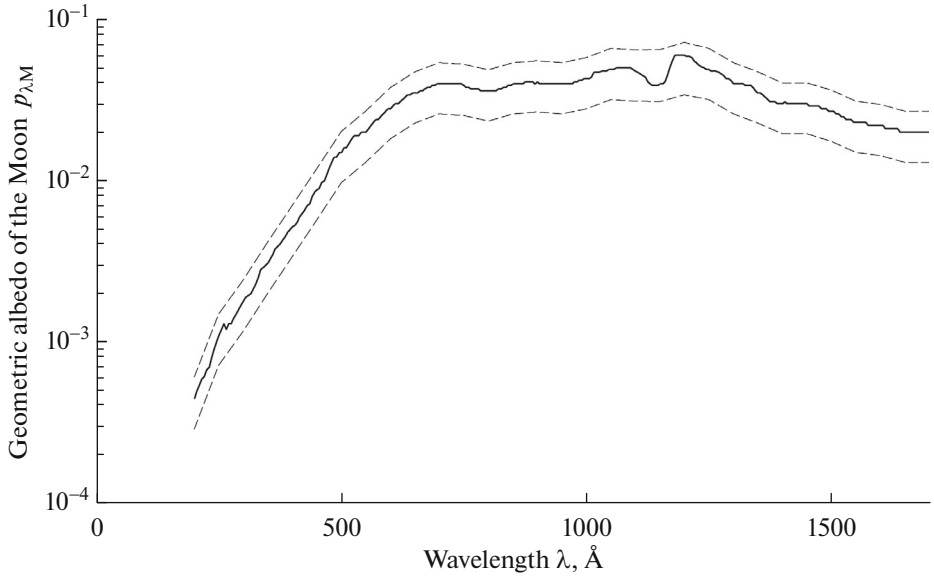

Fig. 1.

the approximation [19] and our digitization. Deviations in Fig. 1 from the monotonicity of the $p_{\lambda M}$ curve within the range of $\lambda = 700–1300$ Å correspond to specific features of the approximation of the geometric albedo of the full moon in original work [19], which are related to a choice of the oxide combination, i.e., 17% Al_2O_3 and 83% SiO_2.

We note that, in [16, 17, 19–23], no explicit formulation of the notion of *geometric albedo* as it is employed by the authors is given, while in the scientific literature, e.g., [8, 11, 27], terms that differ from the viewpoint of physical optics are used to define this notion. Let us dwell upon the consideration of this issue a little bit more.

A geometric albedo by definition [11, 27] is a ratio of the real brightness, i.e., irradiance, of the Moon to the brightness of the absolutely white screen of the same radius located perpendicular to incident solar rays with the phase angle of the Moon $\alpha = 0$ and at the same distances from the Sun and from the observer. In [8], it is stressed that an ideally reflecting Lambertian surface that uniformly scatters in all directions inside the hemisphere, i.e., a solid angle of 2π, is such a screen.

In astrophysics, the term *brightness* is often used instead of the physical term *irradiance*, while the value of the planet's brightness is measured [11, 27] according to the logarithmic scale in star magnitude. In [8], the term *brightness* is used. In [28], when processing the results, the spectral $p_{\lambda M}$ was calculated by the formula $p_{\lambda M} = 4.88 \times 10^4 H_{\lambda M}/H_{\lambda S}$, where $H_{\lambda M}$ and $H_{\lambda S}$ are the spectral irradiances of the full moon and the Sun, respectively. In [17, 19], it is indicated that the method for processing the measurement results is based on simulating the rate of photon counting.

Regardless of the difference in the used terms, in all of the mentioned cases, the value of the geometric albedo $p_{\lambda M}$ (which shows what portion of the incident solar radiation is reflected by the Moon towards the observer compared with that reflected by an ideal flat reflector) is eventually associated with a ratio of fluxes or the flux densities of photons.

The radiation reflected by the Moon is estimated by the irradiance $E_{\lambda M}$, which the Moon creates at the observation point [11], i.e., near the Earth's surface. This value is proportional to the area of the visible lunar disk (projections of a sphere onto the conventional plane) and to the solar irradiance $E_{\lambda S}$, and is inversely proportional to squares of distances from the Sun and from the observer [11]. The irradiance is measured in the energetic units (erg cm^{-2} s^{-1} or photon cm^{-2} s^{-1}). In practice, the value of the solar irradiance $E_{\lambda S}$ at the standard distance equal to one astronomical unit (AU) is used for calculations, since the measurements of the solar radiation flux are conducted near the Earth.

For definiteness, we stress that, in our work, we estimate the spectral irradiance of photon fluxes F_λ of the quantities under study.

3. SOLAR SPECTRAL FLUX IN THE VUV BAND

Spectra of the Sun are presented in numerous monographs and papers (e.g., [29–33]) and by the EUV91 solar spectrum model [18].

A typical spectral irradiance curve of the solar flux $F_{\lambda S}$ (most appropriate to the purpose of our work) for a fairly wide VUV band is given, in particular in [32] (Fig. 1). This is also valuable because it was utilized in the real preflight calibration of the onboard scientific

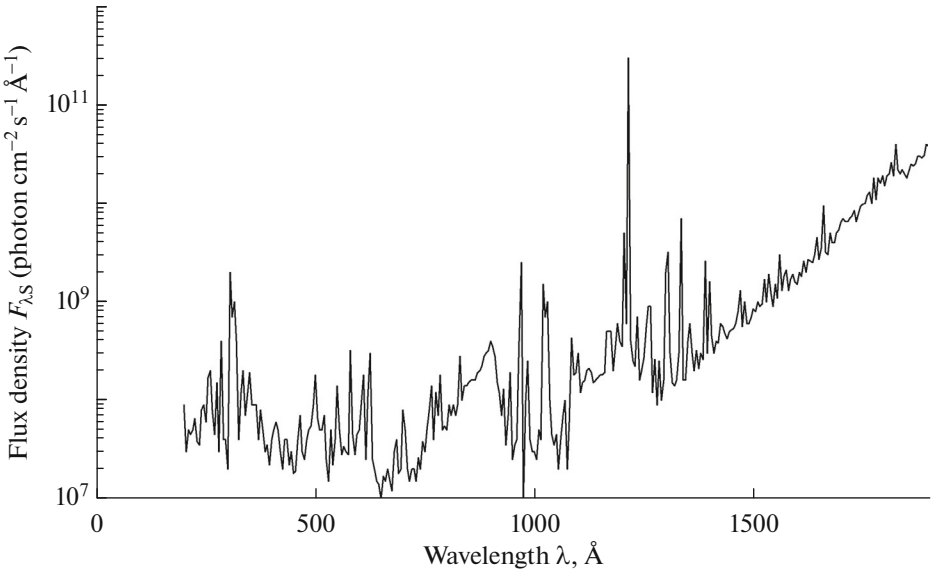

Fig. 2.

instruments in the TIMED (thermosphere, ionosphere, mesosphere energetics and dynamics) mission.

This curve was obtained as a result of complex measurements on October 27, 1992, in the context of the SOLSTICE (solar stellar irradiance comparison experiment) program in the range of 300–1100 Å in rocket experiments and in the range of 1150–1900 Å during the upper atmosphere exploration by UARS (upper-atmosphere research satellite). Spectral resolution of recording these data was better than 4 Å.

The radiation spectrum in the range of $\lambda < 350$ Å was simulated by the radiation of the SURF-III synchrotron of the National Institute of Standards and Technology, United States. This radiation was employed in the preflight ground-based calibration of the unit of silicon photodiodes of the onboard scientific apparatus developed within the TIMED mission.

A photodiode unit with thin-film filters was applied as a set of broadband photometers operating at fixed λ with individual passbands of ~50 Å.

We digitized the spectral curve [32] (Fig. 1) with an error on the order of 10–20% and with a discreteness of around 5 Å and constructed a graph of $F_{\lambda S}$, which is presented in Fig. 2.

With knowledge of the $p_{\lambda M}$ and $F_{\lambda S}$ values, a set of $F_{\lambda I}$ values can be obtained and the spectral irradiance curve of photon flux $F_{\lambda I}$ of the sunlight reflected by the Moon to the ionosphere can be constructed.

4. APPROXIMATION OF THE FLUX DENSITY OF THE VUV RADIATION REFLECTED BY THE FULL MOON ONTO THE EARTH'S IONOSPHERE

An area of the visible disk of the full moon is $S_M = \pi r^2$, where $r = 1737$ km is the radius of the Moon. The solar radiation flux, $\Phi_{\lambda M} = S_M F_{\lambda S} = \pi r^2 F_{\lambda S}$, is incident on this area. During the determination of the geometric albedo $p_{\lambda M}$, the visible disk of the Moon is approximated (see above) as the Lambertian surface scattering the incident solar flux uniformly in all directions of the hemisphere.

The angular size at which the Moon's radius can be seen from the Earth is $r/L \approx 0.0045$ rad. Taking into account that this angle is small, to simplify calculations, the Moon can be assumed to be a point source. With this assumption, an error of estimates of the Earth's illumination by the full moon amounts to roughly 0.002% (in accordance with the inverse-square law [35]), i.e., the ample value for our calculations.

We are interested in the spectral irradiance of the flux $F_{\lambda I}$ reflected by the full moon to the Earth's ionosphere, i.e., at the distance from the Moon $L = 384\,400$ km. At this distance, the area of the hemisphere surface with the Moon's center is $S_L = 2\pi L^2$. Consequently,

$$F_{\lambda I} = p_{\lambda M}\,\Phi_{\lambda M}/S_L = 0.5(r/L)^2 p_{\lambda M} F_{\lambda S} = 1.021 \times 10^{-5}\, p_{\lambda M}\, F_{\lambda S}.$$

Substituting to this formula the digitized values of $p_{\lambda M}$ and $F_{\lambda S}$ for particular λ_i ($i = 1, 2, 3, \ldots$), we constructed a graph of the spectral irradiance of the photon flux $F_{\lambda I}$ presented in Fig. 3.

Below, in Table 1, the values of ionization energies (potentials) E_i for main ionospheric particles, as well as the relevant wavelengths are listed. For the N_2 molecule, a value of dissociation energy additionally is given. The values in Table 1 are rounded to third decimal. In Fig. 3, the ionization wavelengths for main ionospheric atoms and ions are indicated by vertical

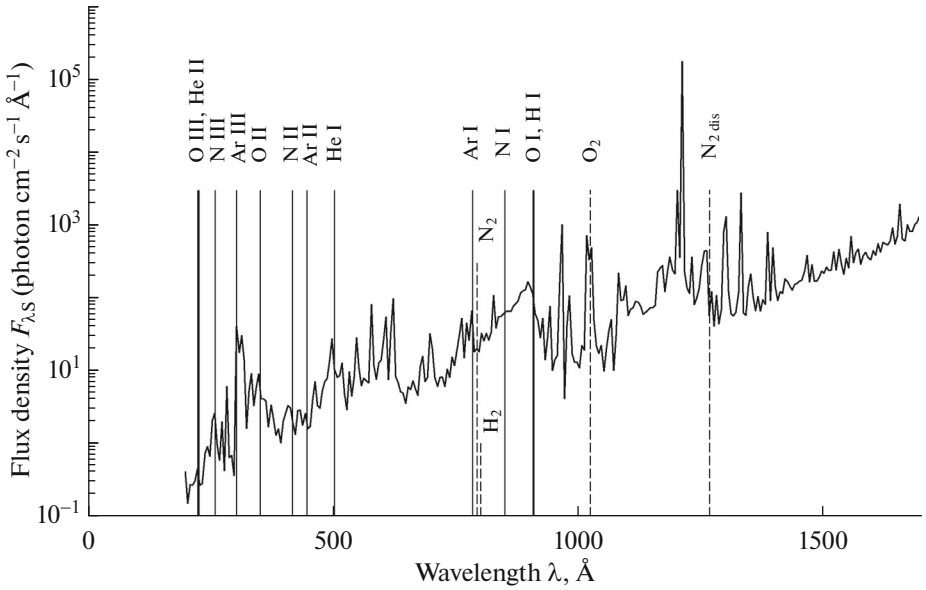

Fig. 3. Vertical solid lines indicate wavelengths of ionization of main ionospheric atoms and ions, while the ionization wavelengths for molecules are shown by dashed lines.

solid lines, while the dashed vertical lines show the wavelengths of ionization for molecules.

It follows from Fig. 3 that, in the VUV radiation reflected by the Moon, there are not only photons, the energies of which are sufficient for ionization of ionospheric particles; in this radiation, there are also photons with energies for exciting the ionospheric particles to the Rydberg states, i.e., to states with high energies that are very close to the ionization energies (this is a subject for our future studies).

Values of spectral irradiance of the flux $F_{\lambda I}$ reflected by the full moon to the Earth's ionosphere in the neighborhoods of ionization energies of main ionospheric particles are given in Table 2.

We note that an error of our estimates of the flux $F_{\lambda I}$ (~35%) depends on the error of initial values of the

Table 1

Particle [Reference]	Ionization energy E_i		Wavelength λ, Å
	eV	cm^{-1}	
O III [36]	54.936	443085.000	225.690
He II [36]	54.418	438908.879	227.838
N III [36]	47.445	382672.000	261.320
Ar III [36]	40.735	328550.000	304.368
O II [36]	35.121	283270.900	353.019
N II [36]	29.601	238750.200	418.848
Ar II [36]	27.630	222848.300	448.736
He I [36]	24.587	198310.666	504.259
Ar I [36]	15.760	127109.842	786.721
N_2 [37]	15.581	125669.246	795.740
H_2 [37]	15.426	124418.280	803.787
N I [36]	14.534	117225.700	853.055
O I [36]	13.618	109837.020	910.440
H I [36]	13.598	109678.772	911.753
O_2 [37]	12.071	78687.450	1027.124
$N_{2\,dis}$ [38]	9.756	78687.450	1270.851

Table 2

Particle	Wavelength λ, Å	Flux F_{IM} (λ), photon cm^{-2} s^{-1} Å^{-1}
O III	225.690	0.3
He II	227.838	0.3
N III	261.320	2
Ar III	304.368	40
O II	353.019	6
N II	418.848	2.5
Ar II	448.736	2
He I	504.259	15
Ar I	786.721	50
N_2	795.740	20
H_2	803.787	20
N I	853.055	60
O I	910.440	90
H I	911.753	90
O_2	1027.124	400
$N_{2\,dis}$	1270.851	105

lunar geometric albedo, which, as was indicated by the authors of [19], did not exceed 30%.

Additionally, the value of the spectral flux density $F_{\lambda I}$ depends on the solar activity and, therefore, the estimates can differ from the values listed in Table 2.

CONCLUSIONS

The approximate spectral curve of $F_{\lambda I}$ presented in Fig. 3, and estimates of maximum values of the flux density $F_{\lambda I}$, given in Table 2, can be used to plan and carry out space experiments.

The data obtained provide an opportunity to estimate of the number of particles in the night ionosphere, i.e., the H I, He I, N I, O I, and Ar I atoms; the He II, N II, O II, Ar II, N III, O III, and Ar III ions; and the H_2, N_2, and O_2 molecules, which are ionized or excited by a part of the Sun's VUV radiation reflected by the full moon towards the Earth's ionosphere.

Spectral resolutions of the initial digitized solar spectrum $F_{\lambda S}$ (see Fig. 2) and, accordingly, spectral flux $F_{\lambda I}$ are not great. By our estimate, they are on the order of 5 Å for $\lambda > 350$ Å. Therefore, when analyzing the excitation and ionization of particles in the night ionosphere, it is necessary to thoroughly select the real (narrower) solar spectral lines for the relevant wavelengths and to take into account their characteristics, such as intensity and half-width. In this case, the solar radiation model for the VUV band can be used [18].

We approximated the spectral irradiance of the flux $F_{\lambda I}$ from the full moon, i.e., the maximum value. Naturally, a decrease in the flux from the Moon depending on its phase should be taken into account, e.g., based on the data presented in [39–41].

In conclusion, we note that studies of the Moon's characteristics in the VUV band continue and remain to be urgent as before [42, 43].

ACKNOWLEDGMENTS

The authors are grateful to O.S. Ugol'nikov for his helpful remarks, which allowed the work to be improved.

REFERENCES

1. Plastinin, Yu.A. and Karabadzhak, G.F., Scientific and applied geophysical experiments *Relaksatsiya*, in *11-aya Mezhdunarodnaya nauchno-prakticheskaya konferentsiya "Nauchnye issledovaniya i eksperimenty na MKS"* (The 11th International Scientific and Practical Conference "Scientific Research and Experiments on the ISS"), Moscow: IKI RAN, 2015, p. 118.
2. Ruzhin, Yu.Ya., Kuznetsov, V.D., Kovalev, V.I., Bershadskaya, I.N., Karabadzhak, G.F., Plastinin, Yu.A., Frolov, V.L., and Parrot M., Observations onboard the ISS Russian segment of auroras and substorm phenomena caused by shortwave radioemission of the SURA heating facility, in *11-aya Mezhdunarodnaya nauchno-prakticheskaya konferentsiya "Nauchnye issledovaniya i eksperimenty na MKS"* (The 11th International Scientific and Practical Conference "Scientific Research and Experiments on the ISS"), Moscow: IKI RAN, 2015, p. 40.
3. Karabadzhak, G.F., Kaleri, A.Yu., Kovalev, V.I., Komrakov, G.P., Kuznetsov, V.D., Plastinin, Yu.A., Ruzhin, Yu.Ya., Frolov, V.L., and Khmelinin, B.A., Observations of global optical and physical phenomena in upper atmospheric layers under the influence of high-power radioemission by heating facility, *Kosmonavtika Raketostroenie*, 2011, vol. 2, pp. 111–118.
4. Ruzhin, Yu.Ya., Kuznetsov, V.D., Kovalev, V.I., Bershadskaya, I.N., Karabadzhak, G.F., Plastinin, Yu.A., Frolov, V.L., Komrakov, G.P., and Parrot M., On the possibility of localization of a substorm by using the "Sura" heating facility, *Radiophys. Quantum Electron.*, 2012, vol. 55, nos. 1–2, pp. 85–94.
5. Ruzhin, Yu.Ya., Kuznetsov, V.D., Plastinin, Yu.A., Karabadzhak, G.F., Frolov, V.L., and Parrot, M., Auroral activity caused by high-power radioemission from the SURA facility, *Geomagn. Aeron. (Engl. Transl.)*, 2013, vol. 53, no. 1, pp. 43–48.
6. Kuznetsov, V.D. and Ruzhin, Yu.Ya., Anthropogenic trigger of substorms and energetic particles precipitations, *Adv. Space Res.*, 2014, vol. 54, no. 12, pp. 2549–2558.
7. Stair, R. and Johnston, R., Ultraviolet spectral radiant energy reflected from the Moon, *J. Res. Natl. Bur. Stand. (U. S.)*, 1953, vol. 51, no. 2, pp. 81–84.
8. Hapke, B., Optical properties of the lunar surface, in *Physics and Astronomy of the Moon*, New York: Academic, 1971, pp. 155–211.
9. Bentley, A.N. and Jonckheere, C.G., Geometric albedo of the Moon in the ultraviolet, *Astron. J.*, 1974, vol. 79, no. 3, pp. 401–403.
10. Wildey, R.L., The lunar geometric albedo and magnitude of the full Moon, *The Observatory*, 1976, vol. 96, pp. 235–239.
11. Shevchenko, V.V., *Sovremennaya selenografiya* (Modern Selenography), Moscow: Nauka GRFML, 1980.
12. Shevchenko, V.V., Main photometric lunar constants in the true full-moon system, *Astron. Zh.*, 1980, vol. 57, no. 6, pp.1341–1343.
13. Shevchenko, V.V., *Luna i ee nablyudenie* (The Moon and Its Observation), Moscow: Nauka, 1983.
14. Henry, R.C., Feldman, P.D., Davidsen, W.K., and Durrance, S.T., Ultraviolet albedo of the Moon with the Hopkins Ultraviolet Telescope, *Astrophys. J.*, 1995, no. 1, pp. L69–L72.
15. Lucey, P.G., Neumann, G.A., Riner, M.A., et al., The global albedo of the Moon at 1064 nm from LOLA, *J. Geophys. Res.: Planets*, 2014, vol. 119, pp. 1665–1679. doi 10.1002/2013JE004592
16. Lucke, R.L., Henry, R.C., and Fastie, W.G., Far-ultraviolet albedo of the Moon, *Astron. J.*, 1976, vol. 81, pp. 1162–1169.
17. Gladstone, G.R., McDonald, J.S., Boyd, W.T., and Bowyer, S., EUVE photometric observations of the

Moon, *Geophys. Res. Lett.*, 1994, vol. 21, no. 6, pp. 461–464.

18. Tobiska, W.K., Revised SERF2 Solar EUV Flux Model 1991. http://cmc.gsfc.nasa.gov/modelweb/sun.
19. Flynn, B.C., Vallerga, J.V., Gladstone, G.R., and Edelstein, J., Lunar reflectivity from extreme ultraviolet explorer imaging and spectroscopy of the full Moon, *Geophys. Res. Lett.*, 1998, vol. 25, no. 17, pp. 3253–3256.
20. Wu, H.H. and Broadfoot, A.L., The extreme ultraviolet albedos of the planet Mercury and of the Moon, *J. Geophys. Res.*, 1977, vol. 82, pp. 759–761.
21. Schmitt, J.H.M.M., Snowden, S.L., Aschenbach, B., et al., A soft x-ray image of the Moon, *Nature*, 1991, vol. 349, pp. 583–587.
22. Henry, R.C., Feldman, P.O., Kruk, J.W., Davidsen, A.F., and Durrance, S.T., Ultraviolet albedo of the Moon with the Hopkins Ultraviolet Telescope, *Astrophys. J.*, 1995, vol. 454, pp. L69–L72.
23. Flynn, B.C., ORFEUS-II far-ultraviolet observations of the lunar atmosphere, *Astrophys. J.*, 1998, vol. 500, pp. L71–L74.
24. Gervais, F., Aluminum oxide (Al_2O_3), in *Handbook of Optical Constants of Solids II*, Palik, E.D., Ed., New York: Academic, 1991, pp. 761–775.
25. Philipp, H.R., Silicon dioxide (SiO_2) (glass), in *Handbook of Optical Constants of Solids*, Palik, E.D., Ed., New York: Academic, 1985, pp. 749–763.
26. Taylor, S.R., *Lunar Science: A Post-Apollo View*, New York: Pergamon, 1975.
27. Martynov, D.Ya., *Kurs obshchei astrofiziki* (A Course of General Astrophysics), Moscow: Nauka GRFML. 1988.
28. Condron, T.P., Lovett, J.J., Barnes, W.H., Marcotte, L., and Nadile, R., *Gemini 7 Lunar Measurements*, Air Force Cambridge Research Laboratory-68-0428, Environmental Research Papers no. 291, 1968.
29. Rottman, G.J., Results from space measurements of solar UV and EUV flux, in *Solar Radiative Output Variation*, Foukal, P., Ed., Boulder: Cambridge Research and Instrumentation Inc., 1987.
30. Ivanov-Kholodnyi, G.S. and Nikol'skii, G.M., *Solntse i ionosfera: Korotkovolnovoe izluchenie Solntsa i ego vozdeistvie na ionosferu* (The Sun and the Ionosphere: Shortwave Solar Radiation and Its Effect on the Ionosphere), Moscow: Nauka, 1969.
31. *Solar Energy Flux and Its Measurements*, White O., Ed., Boulder: Colorado University Press, 1977.
32. Woods, T.N., Rodgers, E.M., Bailey, S.M., Eparvier, F.G., and Ucker, G.J., TIMED solar EUV experiment: Pre-flight calibration results for the XUV photometer system, in *Proc. SPIE*, 1999, vol. 3756, Optical Spectroscopic Techniques and Instrumentation for Atmospheric and Space Research. doi 10.1117/12.366379
33. Phillips, R.J.H., Feldman, U., and Landi, E., *Ultraviolet and X-ray Spectroscopy of the Solar Atmosphere*, Cambridge, 2008.
34. Vazquez, M. and Hanslmeier, A., *Ultraviolet Radiation in the Solar System*, Springer, 2006.
35. Landsberg, G.S., *Optika* (Optics), Moscow: Fizmatlit. 2003.
36. Kramida, A., Ralchenko, Yu., Reader, J., and NIST ASD Team, NIST Atomic Spectra Database (ver. 5.2), Gaithersburg: NIST, 2014. http://physics.nist.gov/asd.
37. *Fizicheskie velichiny: Spravochnik* (Physical Quantities: A Handbook), Grigor'ev, I.S. and Meilikhov, E.Z., Eds., Moscow: Energoatomizdat, 1991.
38. *Spravochnik khimika* (The Chemist's Handbook), Nikol'skii, B.P, Ed., vol. 1, Moscow–Leningrad, Khimiya, 1982.
39. Hapke, B.A., Theoretical photometric function for the lunar surface, *J. Geophys. Res.*, 1963, vol. 68, no. 15, pp. 4571–4568.
40. Hapke, B., An improved theoretical lunar photometric function, *Astron. J.*, 1966, vol. 71, pp. 333–339.
41. Shefov, N.N., Semenov, A.I., and Khomich, V.Yu., *Izluchenie verkhnei atmosfery—indikator ee struktury i dinamiki* (Airglow as an Indicator of Upper Atmospheric Structure and Dynamics), Moscow: GEOS. 2006.
42. Janz, S.J., Hilsenrath, E., Cebula, R.P., and Kelly, T.J., Observations of the lunar geometric albedo during the ATLAS-3 mission, *Geophys. Res. Lett.*, 1996, vol. 23, no. 17, pp. 2297–2300.
43. Taguchi, M., Funabashi, G., Watanabe, S., Takahashi, Y., and Fukunishi, H., Lunar albedo at hydrogen Lyman α by the NOZOMI/UVS, *Earth Planets Space Lett.*, 2000, vol. 52, pp. 645–647.

Translated by M. Samokhina